

International Journal of Scientific Research and Reviews

Satellite And Natural Image Denoising Via Function Approximate And Filter Normalized Butterworth Wavelet

***Purushothaman D. and Chandrasekar C.**

*Department of Computer Science, Dravidian University, kuppam, Andhra Pradesh

Email: aecpurushoth@gmail.com

Department of Computer Science, Periyar University, Salem, Tamil Nadu,

Email : ccsekar@gmail.com

ABSTRACT

Satellite and natural image denoising is significant for strengthening the visual quality of images and for smoothening further image processing and analysis. Designing of filter applying both low pass filters and high pass filters attracted researchers to explore its usefulness in various domains. Furthermore, Wiener filters analyzed the required signal based on the statistical parameters has become a conventional method employed for applications involving image denoising. Thus, reducing noise and improving image visual quality are vital to obtaining better image denoising. In this paper, a novel image denoising method for satellite and natural images, called, Filter Normalized Butterworth Wavelet Frame (FN-BWF) is presented. To start with preprocessing, Function-approximate Discrete Wavelet Transform is applied to the input satellite and natural images with the objective of preserving the edges. Besides, a window centered positioning with function approximation is measured. With the function approximated resultant values, discrete wavelet transform is applied. Finally, image denoising is performed to the edge preserved images by applying Filter Normalized Butterworth Wavelet for the given samples. From the experimental results, it is shown that FN-BWF method significantly minimizes the noise and obtain lower-noise image. The results are compared to two popular denoising methods in the literature, namely Wiener filter based on the Adaptive Cuckoo Search (ACSWF) and Validation of Error Vector Magnitude (VEVM). Results analysis shows that the FN-BWF method performs better than ACSWF and VEVM in terms of peak signal to noise ratio, preprocessing time, average processing time for image denoising and image denoising accuracy.

KEYWORDS: Wiener filters, image denoising, Filter Normalized, Butterworth Wavelet Frame, Function-approximate, Discrete Wavelet Transform.

***Corresponding author**

***Purushothaman D.**

Research Scholar, Department of Computer Science, Dravidian University,

kuppam, Andhra Pradesh,

Email: aecpurushoth@gmail.com

INTRODUCTION

Image denoising is the most prerequisite for improving the image visual quality and for easing further image processing and analysis tasks. Multi Spectral Imagery (MSI) is undeviatingly arising in its reputation as a digital means for sensing remote objects, analysis of terrain, signature detection and so on. Besides, wavelet representations have found suitable place in image denoising due to the reason that the natural images possess a specific statistical behavior in this domain. On the one hand, smoothness is denoted according to the strong energy compaction in coarse scales, while the integration of smooth regions with local, gives rise to sparse activation of wavelet sensors.

Wiener filter based on the Adaptive Cuckoo Search (ACSWF) ¹ as designed with the objective of denoising multispectral satellite images polluted with the Gaussian noise of several dissimilarity extents. The ACS algorithm was proposed for optimizing the Wiener weights. This was done so that the best probable calculations of the desired uncorrupted image could be obtained. To substantiate the performance and computational capability of ACSWF, both quantitative and qualitative comparisons were made.

The key idea of the ACSWF method was to identify the best probable estimate of the original image. This was done via 2-D Finite Impulse Response (FIR) Wiener filtering. The 2-D FIR Wiener filter was designed in such a manner so that the window weights were modified in an adaptive manner. Further, the mean square error (MSE) between the desired image and the filter output was also investigated. Besides, the least possible mean squared error was ensured using the ACS algorithm that in turn optimizes filter weights. With this method, both the computational time and error was found to be significantly minimized while denoising satellite images. However, less focus was made on the image denoising accuracy.

Many notable images comprises certain amount of noise, contains some extent of noise, which are either unaccountable or out of interest. If the noise present in these images is filtered, the process of image analysis is then said to be simplified. Validation of Error Vector Magnitude (EVM) using Butterworth and Chebyshev Filters to differentiate filters responding to industrial requirements in terms of time and cost was presented in². The designing of the method was based on the Quadrature Phase Shift Keying (QPSK) that was sent through the Radio Frequency (RF) device, with the output being the frequency domain and time domain. With this method, the response time was found to be reduced with higher sensitivity to error for RF device performance.

In this paper, two novel solutions for satellite and natural image denoising are proposed. In the first solution, a window centered positioning is used as the basis to extract the slope values with which function approximation is performed for each samples with the aid of discrete wavelet

transform to minimizing the time while preserving the edges during preprocessing. In the second solution, with the edge preserved image given as input, a high pass filter employing Butterworth with Filter Normalization is applied to minimize the noise. With these function approximate filter normalization, the image denoising quality is said to be improved.

The major contributions of this work are summarized as below.

- The proposed Filter Normalized Butterworth Wavelet Frame (FN-BWF) method transforms to noisy satellite and natural images minimize the noise with higher accuracy rate. At first, the input noisy satellite and natural images are converted into edge preserved images in the preprocessing step. The FN-BWF method with the aid of slope values during preprocessing to preserve the edge based on the function approximation. The application of function approximation minimizes the preprocessing time.
- The Filter Normalized Butterworth Wavelet Frame performs the image sharpening based on the cut off frequency obtained through Mutual Information. Based on the mutual information factor, the cut off frequency is arrived. Finally, image denoising is then performed by applying the Butterworth Wavelet Frame via high pass filter, resulting in minimizes the noise and improves the image denoising accuracy.

The rest of this paper is organized as follows: Section 2 provides related works on Image Denoising methods provided by different researchers. Section 3 proposes Filter Normalized Butterworth Wavelet Frame (FN-BWF) transforms to noisy satellite and natural images. In Section 4, experimental settings for the FN-BWF method are presented. In Section 5, the discussion with the table values and graph form is presented. Finally, Section 6 concludes the work.

RELATED WORKS

The application of partial differential equations has been largely studied in the literature due to their significant advantages in both theory and computation. In ⁵, a novel fractional diffusion-wave equation with non-local regularization method was applied for noise removal to enhance image structure. However, the images selected for denoising was found to be static.

To address dynamic images, Non-local Maximum Likelihood (NML) method was applied in ⁶ where the samples were collected in an adaptive manner. Here, not only dynamic images were applied, image denoising was also performed in a significant manner. But, self-similarity test was not said to be ensured. To address this issue, rough set image based denoising was used in ⁷, resulting in the improvement of denoising accuracy.

However, artifacts in denoised images were introduced due to the optimization techniques used in the previous works. In ⁸, an Evolved Local Adaptive (ELA) model was applied to perform

natural image denoising. During the training process, a patch clustering model was deployed. Followed by which, genetic programming was applied for obtaining the optimal filter, therefore ensuring computational efficiency.

Yet another image denoising method by applying Additive White Gaussian Noise (AWGN) model was introduced in ⁹ with the objective of improving peak signal to noise ratio. Despite accuracy and noise being improved, the computational time involved was not focused in the above said methods. To address this issue, discrete wavelet transform (DWT) was applied in¹⁰, therefore minimizing the computational time involved during preprocessing.

Noise includes a random variation of color in image or otherwise referred to as the unwanted signals. The noise gets amalgamated with the original image, causing several troubles. As a result, with the presence of noise, image quality gets deteriorated affecting the edge sharpness and pattern recognition.

In¹¹, a hybridization technique was applied to reduce the peak signal to noise ratio. However, the edge enhancement was said to be badly affected. To address this issue, in ¹², adaptive wavelet threshold shrinkage algorithm was applied to the color image, therefore resulting in superior color image denoising. In the current few years, the discriminative model learning for image denoising receiving attentions owing to its higher denoising performance.

In ¹³, feed-forward denoising convolutional neural networks (DnCNNs) was investigated that involved very deep architecture, learning algorithm, and regularization method to achieve efficient image denoising. Besides, in DnNNs, residual learning and batch normalization were applied for higher convergence and improve the denoising performance.

Yet another structure-based low rank method with graph nuclear normalization was investigated in ¹⁴ with the objective of performing Gaussian noise removal and mixed noise removal by applying local manifold structure. An extension of the Non-Local Means denoising method was investigated in ¹⁵ that used affine invariant self-similarities with the aid of real scenes. A better image denoising was said to be ensured by undergoing a transformation.

Restructure the image that has been corrupted by Additive White Gaussian Noise (AWGN) and Impulse Noise (IN) is considered to be the most challenging issues to be handled due to its complications of the mixture noise. Several research works have been focused to initially identify the impulse noise location and then to restructure the clean image. In ¹⁶, an integrated noise removal model was designed on the basis of Laplacian Scale Mixture (LSM) and nonlocal low-rank regularization therefore adaptively characterizing the real noise.

Yet another image denoising method was introduced in ¹⁷ by applying complex valued wavelet transform, therefore ensuring both quantitative and visual performance. Several research

works have been conducted for image denoising that not only suppresses the noise but also preserve the edge details. In ¹⁸, a constrained optimization approach was applied that combined multiple Non Local Means algorithm that greatly minimized parameter sensitivity and also improving the performance of denoising capacity. Yet another traffic image denoising was investigated in ¹⁹ using neighbourhood weight interpolation algorithm.

The process of filtering out unwanted frequencies is referred to as filtering. The purpose of applying filtering for the given image is to process the image in such a manner that the image becomes more apt than the original image given as input. Besides, image filtering also involves the process of noise removal. In ²⁰, image denoising was performed by applying Butterworth High Pass filter that not only removed the noise but also minimizing the time for noise removal.

In this paper, we present an image denoising method for satellite and natural images based on the filtering algorithm. First, we use the Function-approximate Discrete Wavelet Transform to perform preprocessing so that edges are said to be preserved during the preprocessing state with minimum time and accuracy. Followed by this, with the edge preserved preprocessing satellite and natural images, Filter Normalized Butterworth Wavelet Frame is applied to denoise the image.

FILTER NORMALIZED BUTTERWORTH WAVELET FRAME TRANSFORMS TO SATELLITE AND NATURAL IMAGES

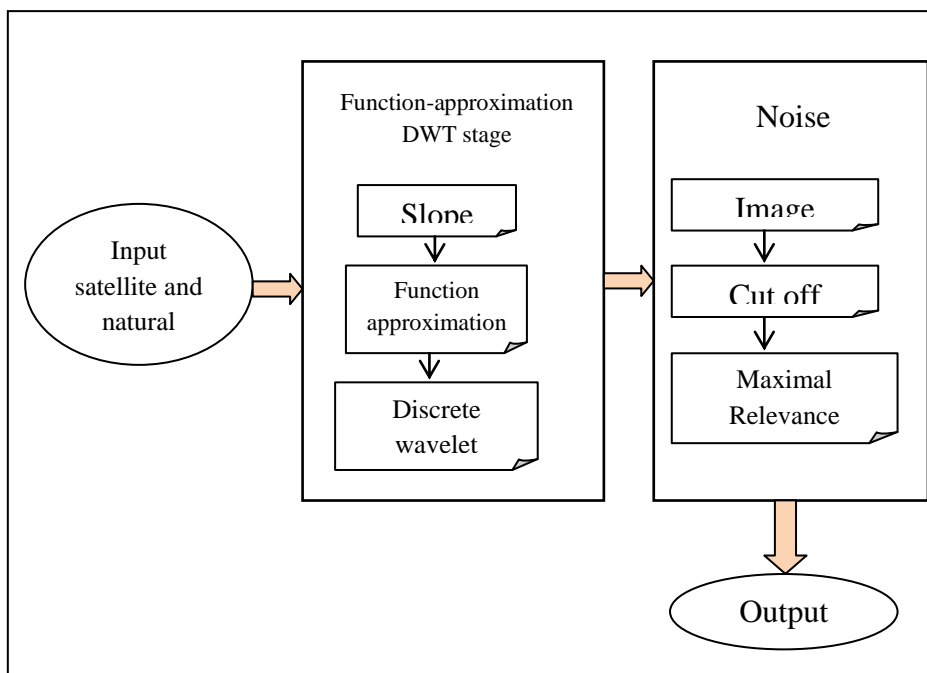
In this paper, we present a new denoising method, which is based on the application of the Filter Normalized Butterworth Wavelet Frame (FN-BWF) transforms to noisy images. A family of statistical parameters for optimizing weight vectors in the space of obtaining best possible estimate of the original image belonging to the satellite images was presented in¹. These frames, which are related to Wiener filters, were derived for ensuring the least possible mean square error. Though errors were reduced, the time consumed was found to be arbitrarily high. The filtering in¹ was implemented in a linear mode. In this paper, we modify this construction in order to use the Function-approximate Discrete Wavelet Transform (FDWT). This modification adds flexibility to the implementation and enables to normalize the filtering functions without compromising the computational time involved during normalization.

The idea behind the filter normalization is as given below. The application of the image sharpening filters optimizes the numerical differentiation by different orders. Typically, this image sharpening filter enhances the noise factor. These image sharpening filters is modified using a method that is based on Mutual Information⁴. The denoising procedure consists of subsequent application of the maximum relevancy and minimum redundancy between two pixel points according to the cut off frequency or threshold factor. Hence, the subsequent processing function is

said to be linear. As a result, significant noise suppression is said to be achieved while retaining the coherent structure of the image without creating artifacts.

Motivated in part by Wiener filters and image pyramids and Butterworth, a novel image denoising method, called Filter Normalized Butterworth Wavelet Frame (FN-BWF) transforms is presented. Figure 1 show the proposed FN-BWF method with its two stages.

Figure 1 proposed Filter Normalized Butterworth Wavelet Frame



1. In the function approximate discrete wavelet stage, degree of certain pixel is first used to convert logarithmical transformation to obtain up, down, left and right slope values is first used to extract the edge detected images with less time and computational overhead. Then, a function approximation is applied to the original image and noise. To this, a discrete wavelet transform is applied wherein the edges of the input images (i.e. noisy images) are said to be preserved during preprocessing.
2. In the noise reduction stage, image sharpening is said to be performed by applying appropriate filter, called Filter Normalized Butterworth. A cut off frequency with mutual information is applied to the images for reducing the noise (i.e. image denoising) present in the images.
3. The combination of function approximation followed by filter normalizing procedure yields the noise reduction in satellite and natural images.

The above stages are formulated in detail in the following subsection.

a. Function-approximate Discrete Wavelet Transform preprocessing model

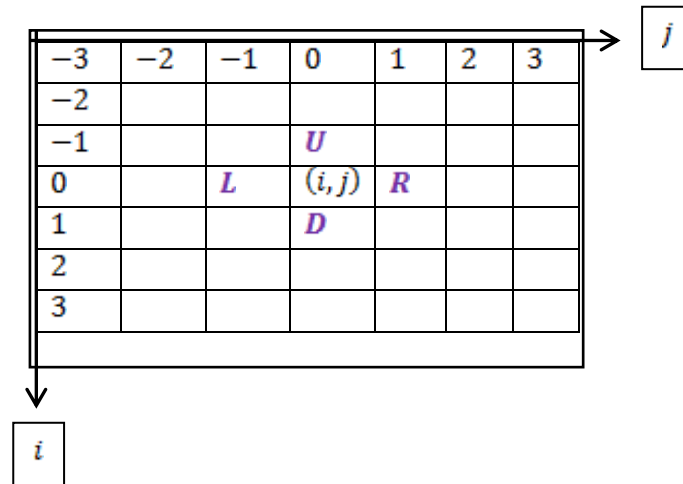
In this work, Function-approximate Discrete Wavelet Transform (FDWT) preprocessing model is applied to the noisy image with the objective of not only minimizing the computational time

during preprocessing but also to preserve the edges during preprocessing. To achieve this objective, the preprocessing model in this work, includes a function-approximate with respect to a projection range ‘ α ’ for ‘ k ’ samples. Followed by this, a Discrete Wavelet Transform is applied to the approximated function value to restore the edges during preprocessing.

The satellite ¹ and natural images ³ are frequently corrupted by noise due to several factors, to name a few, being, image acquisition device, acquisition time and hence certain pixel values are certainly corrupted whereas certain other pixel values remain free from noise. However, while removing the noise, the edge should be preserved. In this work, not only noise removal is performed but also the edges of the noisy images are preserved, into account, therefore improving the image denoising accuracy.

In this work, a noisy image ‘ NI ’ with size ‘ $M * N$ ’ pixels are extracted directly from satellite¹ and natural³ images and ‘ $ni(i, j)$ ($1 \leq i \leq M, 1 \leq j \leq N$)’ represents the pixel value at location ‘ (i, j) ’. In order to determine whether the pixel ‘ $ni(i, j)$ ’ is corrupted with noise, a window centered at ‘ $ni(i, j)$ ’ is represented as ‘ $W(i, j)$ ’, i.e., ‘ $W(i, j) = \{ni(i - l, j - s)\}$ ’ as illustrated in figure 2.

Figure 2 : Window centered positioning



As illustrated in the figure 2, for developing the noise detection, in the window ‘ $W(i, j)$ ’, the degree of certain pixel ‘ $ni(i, j)$ ’ considered as noise. The four neighbors of ‘ $ni(i, j)$ ’ correlates to the directions ‘Up (U), Down (D), Left (L), Right (R)’ respectively. With this the slope values ‘ $MU(i, j), MD(i, j), ML(i, j), MR(i, j)$ ’ and ‘ $ni(i, j)$ ’ of pixel values ‘ (i, j) ’ is mathematically measured as given below.

$$MU(i, j) = ni(i + 1, j) - ni(i, j) \tag{1}$$

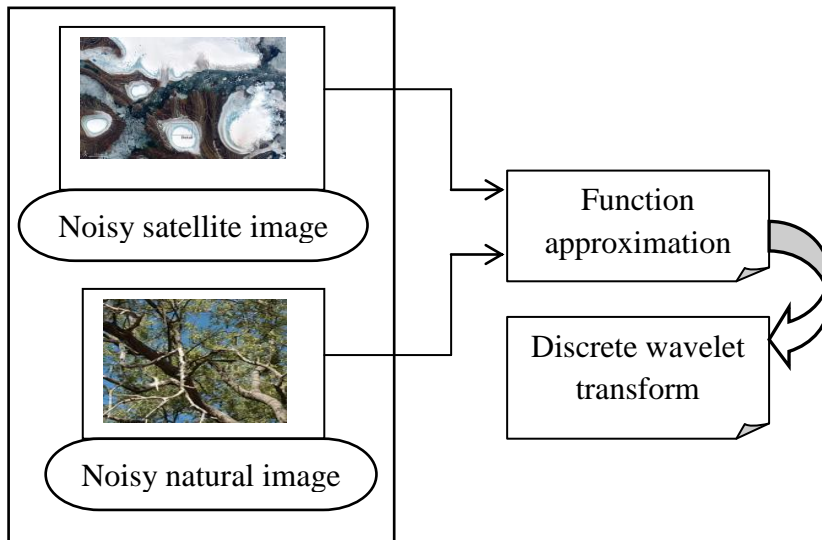
$$MD(i, j) = ni(i, j + 1) - ni(i, j) \tag{2}$$

$$ML(i, j) = ni(i + 1, j) - ni(i, j) \tag{3}$$

$$MR(i,j) = ni(i,j - 1) - ni(i,j) \tag{4}$$

From the above equations (1), (2), (3) and (4), ‘ $MU(i,j)$ ’, ‘ $MD(i,j)$ ’, ‘ $ML(i,j)$ ’ and ‘ $MR(i,j)$ ’ represents the mean values of the pixel ‘ $ni(i,j)$ ’. Figure 3 shows the Function-approximate Discrete Wavelet Transform (FDWT) preprocessing model.

Figure 3 Function-approximate Discrete Wavelet Transform preprocessing model



As illustrated in the figure, with the noisy images obtained from the satellite and natural images, instead of obtaining the function value for any given set of images (i.e. samples) that is found to be time consuming process, the approximation function in this work measure one single function value. By including an approximation function, the computational time is said to be reduced. Therefore, a function-approximate DWT exploited in this work. It is mathematically expressed as given below.

$$FA(i,j) = OI(i,j) + \rho(i,j) \tag{5}$$

From the above equation (5), ‘ $FA(i,j)$ ’ represents the approximation function of pixel values ‘ (i,j) ’, being a summation of the original image ‘ OI ’ and noise ‘ ρ ’ with pixel values ‘ (i,j) ’ respectively. With the function approximate resultant values, the discrete wavelet transform for ‘ k ’ samples is obtained and is mathematically formulated as given below.

$$WFA(\alpha,k) = 2^{-\alpha} \sum_{\rho=1}^N FA(\rho)(2^{-\alpha} \rho - k) \tag{6}$$

From the above equation (6), the function approximate ‘ FA ’ with discrete wavelet ‘ W ’ and projection range ‘ α ’ for ‘ k ’ samples is obtained using the function approximate noised values ‘ $FA(\rho)$ ’ with respect to the overall samples. The pseudo code representation of Function-approximate Discrete Wavelet Transform (FDWT) edge detection is given below.

Algorithm 1 Function-approximate Discrete Wavelet Transform (FDWT) edge detection

<p>Input: Original Image '$OI(i,j)$', Noisy Image '$NI(i,j)$', size '$M * N$' pixels, samples 'k', noise 'ρ', projection range 'α'</p>
<p>Output: Edge preserved image detection '$EPI(i,j)$'</p>
<p style="text-align: center;">1: Begin</p> <p>2: For each noisy image '$NI(i,j)$' with window '$W(i,j)$' for 'k' samples</p> <p style="padding-left: 40px;">3: For pixel value at location '$ni(i,j)$'</p> <p style="padding-left: 80px;">4: Measure the up slope values using equation (1)</p> <p style="padding-left: 80px;">5: Measure the down slope values using equation (2)</p> <p style="padding-left: 80px;">6: Measure the left slope values using equation (3)</p> <p style="padding-left: 80px;">7: Measure the right slope values using equation (4)</p> <p style="padding-left: 80px;">8: Obtain function-approximate using equation (5)</p> <p style="padding-left: 40px;">9: Obtain discrete wavelet transform for 'k' samples using equation (6)</p> <p style="padding-left: 80px;">10: End for</p> <p style="padding-left: 40px;">11: End for</p> <p style="text-align: center;">12: End</p>

As given in the above FDWT algorithm, for each noisy image ' $NI(i,j)$ ' with window ' $W(i,j)$ ' and ' k ' samples considered as input, the objective of the algorithm remains in preserving the edges of the input satellite and natural images during preprocessing. To achieve this objective, for each image corrupted with noise at pixel location ' $ni(i,j)$ ', the corresponding slope values towards the upward, downward, left and right direction are measured. With this, the edges of the input images (i.e. noisy images) are said to be preserved during preprocessing. Followed by this slope intercept identification, function approximate is done. The purpose of using the function approximate is rather than using the entire slope intercept values for a single noisy image, an approximated value is used so that the computation time involved during preprocessing is said to be reduced.

FILTER NORMALIZED BUTTERWORTH WAVELET

In order to reduce the noise present in the natural and aerial images, the most prerequisite is the appropriate selection of correct filtering function. Different filter types exist according to the preprocessed images. In this work, the focus behind preprocessing remains in preserving the edges, so Butterworth Filter is applied to the edge preserved images. Besides, image sharpening is performed that in turn emphasizes fine tuned image. Hence, to start with, image sharpening is performed with it, is mathematical formulation as given below.

$$H(i, j) = 0; \text{ if } Dis(i, j) \leq \beta \tag{7}$$

$$H(i, j) = 1; \text{ if } Dis(i, j) > \beta \tag{8}$$

From the above two equations (7) and (8), ‘ β ’ represents the cut off frequency (i.e. threshold factor) used to measure the adjacent pixels according to the distance ‘ Dis ’ between the pixel values ‘ i ’ and ‘ j ’. The cut off frequency or the threshold factor to measure the adjacent pixels is selected in this work based on the mutual information⁴. It is mathematically represented as given below.

$$\beta = MI(j, i') - \gamma \sum_{OI \in \varphi} MI(i', OI(i, j)) \tag{9}$$

From the above equation (9), the mutual information for the cut off frequency is obtained according to the binary terms. The first term ‘ $MI(j, i')$ ’ in the above equation (i, j) maximizes the relevancy of ‘ i' ’ to ‘ j ’. The second term ‘ $MI(i', OI(i, j))$ ’ in the above equation (i, j) minimizes the redundancy between ‘ i' ’ and the already selected original image ‘ $OI(i, j)$ ’. The balance between maximum relevancy and minimum redundancy is obtained via by the parameter ‘ γ ’. Figure shows the resultant sharpened image for the edge preserved image via mutual information factor.

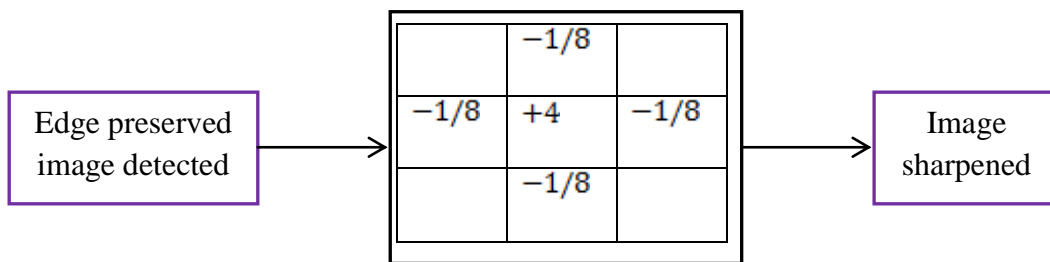


Figure 4 Image sharpening for edge preserved image

As shown in the above figure, the adjacent pixels for the corresponding origin are represented by the minus sign. With no changes in the intensity of the edge preserved image, nothing is said to occur. On the other hand, if one pixel value is brighter than its adjacent pixels, the corresponding pixel value is said to be boosted. Finally, the function normalized (i.e. normalization of cut off frequency) of Butterworth high pas filter with cut off frequency ‘ β ’ and order ‘ n ’ is mathematically represented as given below.

$$H(i, j) = \frac{1}{1 + \left[\frac{\beta}{Dis(i, j)} \right]^{2n}} \tag{10}$$

From the above equation (10), ‘ $Dis(i, j)$ ’ represents the distance between the two pixel points ‘ (i, j) ’ to the center of the origin with ‘ β ’ representing the cutoff range from the origin. Then, the distance between the two pixel points ‘ (i, j) ’ with rows ‘ M ’ and columns ‘ N ’ is mathematically formulated as given below.

$$Dis(i, j) = \left(i - \frac{M}{2}\right)^2 + \left(j - \frac{N}{2}\right)^2 \quad (11)$$

The pseudo code representation of Filter Normalized Butterworth Image Denoising is given below.

Algorithm 2 Filter Normalized Butterworth Image Denoising algorithm

Input: Edge preserved image ‘ $EPI(i, j)$ ’, cut off frequency ‘ β ’, rows ‘ M ’, columns ‘ N ’
Output: Denoised images (Satellite and natural image)
<p style="text-align: center;">1: Begin</p> <p style="text-align: center;">2: For each Edge preserved image ‘$EPI(i, j)$’</p> <p style="text-align: center;">3: Perform image sharpening using equation (7) and (8)</p> <p style="text-align: center;">4: Measure cut off frequency using equation (9)</p> <p style="text-align: center;">5: Measure function normalization using equation (10)</p> <p style="text-align: center;">6: End for</p> <p style="text-align: center;">7: End</p>

As given in the above algorithm, with edge preserved image given as input, the objective of Filter Normalized Butterworth Image Denoising (FNBID) algorithm remains in denoising the image with higher accuracy and minimum time. These two objectives are said to be achieved by applying a filter normalized butterworth model. Initially, normalization of cut off frequency is evaluated. With this normalized cut off frequency, Butterworth high pass filter is applied to the input edge preserved image. With this image denoising is said to be achieved with higher accuracy, as because, instead of using the cut off factor in a random manner, a normalization factor is said to be found. This in turn improves the image denoising accuracy with minimum time consumption.

EXPERIMENTAL SETTINGS

In this section, a series of experiments are conducted to verify the efficiency and effectiveness of our image denoising algorithm. For comparison, Wiener filter based on the Adaptive Cuckoo Search (ACSWF)¹ and Validation of Error Vector Magnitude (Validation of EVM)² are chosen for image denoising. Tests are conducted using satellite¹ and natural images³ database.

The satellite images are procured from several sources, such as Satpalda Geospatial Services, Satellite Imaging Corporation, and NASA. All the test images included in the study are MS images with four bands (blue: 430–550 nm; green: 500–620 nm; red: 590–710 nm; near IR: 740–940 nm). The natural images are selected from UPenn Natural Image Database, that include many snapshots of what a human observer might conceivably look at, such as images of the horizon and detailed images

of the ground, trees, bushes, and baboons and the defined testing method results are compared with existing method.

The natural images were obtained from³. In order to perform image denoising with satellite and natural images, the proposed Filter Normalized Butterworth Wavelet Frame (FN-BWF) method is compared with two other existing methods, ACSWF¹ and Validation of EVM² using satellite and natural images. Experimental evaluation using FN-BWF method is conducted on various factors such as PSNR, average processing time (i.e. for image denoising) and image denoising accuracy with respect to different satellite and natural images.

DISCUSSION

To validate the efficiency and theoretical advantages of the Filter Normalized Butterworth Wavelet Frame (FN-BWF) method for image denoising using satellite and natural images with ACSWF¹ and Validation of EVM² performance evaluation results are presented. The parameters of the FN-BWF method are chosen as provided in the experiment section.

IMPACT OF PSNR

To measure the performance of FN-BWF method, three experiments are conducted. The first one is designed to measure the noise ratio caused by noisy satellite and natural images. One of the simplest ways to measure the noise during image denoising for satellite and natural images is measuring PSNR. Higher value of PSNR indicates higher natural image quality. The noise factor is measured according to the size of satellite and natural image in pixels. With denoising to be performed for satellite and natural images, it is analogous that a significant amount of noise is added to it. Besides, the noise should be imperceptible by Human Visual System (HVS). PSNR is used to measure the quality of the satellite and natural images. PSNR is mathematically formulated as given below.

$$PSNR = 10 \log_{10} \left(\frac{L^2}{MSE} \right) \quad (12)$$

From the above equation (12), ' L ' represents the peak signal level, whereas ' MSE ' represents the Mean Squared Error²¹, which is the pixel value of the image. The value of MSE is mathematically formulated as given below.

$$MSE = \left[\frac{1}{k \times k} \right] \sum_{i=1}^n \sum_{j=1}^n [OI(i-j) - NI(i-j)]^2 \quad (13)$$

Where ' $OI(i, j)$ ' and ' $B(i, j)$ ' are the pixel intensity values of the original image and the noisy image respectively and ' k ' represents the size of input satellite and natural images. The sample calculation followed by graphical representation is given below.

Sample calculation

- **Proposed FN-BWF:** With single (i.e. satellite) image given as input, the value of MSE being ‘350’, the PSNR is mathematically evaluated as given below. Then for ‘10’ images given as input, the PSNR is found to be ‘85.7dB’. In a similar manner, with single (i.e. natural) image given as input, the value of MSE being ‘300’, the PSNR is mathematically evaluated as given below. Then for ‘10’ images given as input, the PSNR is found to be ‘92.9dB’.

$$PSNR \text{ (using satellite image)} = 10 \log(10) * \frac{255}{350} = 8.57dB$$

$$PSNR \text{ (using natural image)} = 10 \log(10) * \frac{255}{300} = 9.29dB$$

- **ACSWF:** With single (i.e. satellite) image given as input, the value of MSE being ‘450’, the PSNR is mathematically evaluated as given below. Then for ‘10’ images given as input, the PSNR is found to be ‘74.8dB’. In a similar manner, with single (i.e. natural) image given as input, the value of MSE being ‘400’, the PSNR is mathematically evaluated as given below. Then for ‘10’ images given as input, the PSNR is found to be ‘80.49dB’.

$$PSNR \text{ (using satellite image)} = 10 \log(10) * \frac{255}{450} = 7.48dB$$

$$PSNR \text{ (using natural image)} = 10 \log(10) * \frac{255}{400} = 8.04dB$$

- **Validation of EVM:** With single (i.e. satellite) image given as input, the value of MSE being ‘550’, the PSNR is mathematically evaluated as given below. Then for ‘10’ images given as input, the PSNR is found to be ‘66.3dB’. In a similar manner, with single (i.e. natural) image given as input, the value of MSE being ‘500’, the PSNR is mathematically evaluated as given below. Then for ‘10’ images given as input, the PSNR is found to be ‘70.7dB’.

$$PSNR \text{ (using satellite image)} = 10 \log(10) * \frac{255}{550} = 6.62 dB$$

$$PSNR \text{ (using natural image)} = 10 \log(10) * \frac{255}{500} = 7.07dB$$

Table 1 PSNR using Satellite and Natural images

No. of images	PSNR (using satellite images)			PSNR (using natural images)		
	FN-BWF	ACSWF	Validation of EVM	FN-BWF	ACSWF	Validation of EVM
10	85.7	74.8	66.3	92.9	80.49	70.7
20	90.4	77.5	69.4	92.5	82.4	75.3
30	91.3	80.2	70.2	93.2	84.3	79.4
40	94.2	83.4	75.3	96.5	89.1	80.5
50	96.5	85.5	80.4	98.3	80.3	78.4

60	85.4	75.2	70.2	87.1	82.5	74.3
70	89.1	80.4	75.4	91.6	84.2	76.1
80	90.4	85.3	80.1	92.3	86.3	85.4
90	85.4	82.4	76.3	87.2	80.2	72.3
100	90.4	85.5	77.1	88.4	84.1	71.5

Table 1 given above presents the PSNR rate with respect to 100 different numbers of satellite and natural images used. From this table it is inferred that the PSNR rate is improved using the proposed FN-BWF method when applied with two different satellite and natural images. Several images are present in both the satellite and natural images, among them, 100 images are taken for observation. The PSNR is found to be higher when applied with the proposed FN-BWF method than ACSWF¹ and Validation of EVM² respectively. This is because of the application of Filter Normalized Butterworth Wavelet Frame in the FN-BWF method that filters the noisy portions and therefore improving the rate of PSNR. First, image sharpening is performed using mutual information. By performing image sharpening, the edge preserved images appear to be more defined by darkening the darker portions of images and brightening the brighter portions of images. As a result, the contrast of the image is said to be improved when applied with both satellite and natural images. Second, the cut off frequency is not selected in a random manner, but mutual information between the images and the adjacent pixels of the given input noisy satellite or natural images are used. This in turn improves the PSNR rate when both satellite and natural noisy images are provided as input. With regard to the obtained results, the experiment with the best performance is FN-BWF method achieving PSNR greater than 11% compared to ACSWF¹ and 22% compared to Validation of EVM² with satellite images as input and 10% compared to ACSWF¹ and 21% compared to Validation of EVM² with natural images as input.

a. Impact of average processing time

The performance results in previous section have indicated that FN-BWF method is more effective than ACSWF and Validation of EVM in terms of PSNR. In this section, a comparative analysis of FN-BWF method with ACSWF and Validation of EVM is evaluated to measure the performance of average processing time. The average processing time measures the average time required to process an image (i.e. preprocessing and image denoising). The average processing time is the summation of time taken to preserve edge (i.e. preprocessing) and noise removal (i.e. image denoising). It is mathematically formulated as given below.

$$AP_{time} = k * Time (FDWT) + Time (FNBID) \tag{14}$$

From the above equation (14), the average processing time ‘ AP_{time} ’ is obtained by applying the time taken for preprocessing ‘ $Time (FDWT)$ ’ and time taken for denoising ‘ $Time (FNBID)$ ’

respectively with respect to the samples ‘*k*’ provided as input. It is measured in terms of milliseconds (ms). The sample calculation is provided below, followed by which graphical representation is included.

Sample calculation

- **Proposed FN-BWF:** With ‘10’ satellite images given as input, the time consumed for preprocessing being ‘0.035ms’ and image denoising being ‘0.132ms’, the average preprocessing time is ‘1.67ms’. In a similar manner, with ‘10’ natural images given as input, the time consumed for preprocessing being ‘0.039ms’ and image denoising being ‘0.145ms’, the average preprocessing time is ‘1.84ms’.

$$AP_{time}(\text{using satellite image}) = 10 * [0.035ms + 0.132ms] = 1.67ms$$

$$AP_{time}(\text{using natural image}) = 10 * [0.039ms + 0.145ms] = 1.84ms$$

- **ACSWF:** With ‘10’ satellite images given as input, the time consumed for preprocessing being ‘0.045ms’ and image denoising being ‘0.155ms’, the average preprocessing time is ‘2ms’. In a similar manner, with ‘10’ natural images given as input, the time consumed for preprocessing being ‘0.055ms’ and image denoising being ‘0.175ms’, the average preprocessing time is ‘2.3ms’.

$$AP_{time} = 10 * [0.045ms + 0.155ms] = 2ms$$

$$AP_{time} = 10 * [0.055ms + 0.175ms] = 2.3ms$$

- **Validation of EVM:** With ‘10’ satellite images given as input, the time consumed for preprocessing being ‘0.058ms’ and image denoising being ‘0.170ms’, the average preprocessing time is ‘2.27ms’. In a similar manner, with ‘10’ natural images given as input, the time consumed for preprocessing being ‘0.069ms’ and image denoising being ‘0.189ms’, the average preprocessing time is ‘2.58ms’.

$$AP_{time} = 10 * [0.058ms + 0.170ms] = 2.27ms$$

$$AP_{time} = 10 * [0.069ms + 0.189ms] = 2.58ms$$

Table 2 Average processing time

No. of images	Average processing time (using satellite images)			Average processing time (using natural images)		
	FN-BWF	ACSWF	Validation of EVM	FN-BWF	ACSWF	Validation of EVM
10	1.67	2	2.27	1.84	2.3	2.58
20	2.55	3.25	5.55	2.85	4.55	6.55
30	4.89	5.66	7.85	5.66	6.89	8.95
40	6.55	8.55	10.45	8.35	10.25	14.55

50	8.23	10.32	12.55	10.35	15.55	16.75
60	7.45	8.15	15.55	12.25	18.25	20.32
70	9.52	12.35	13.52	11.45	16.75	18.55
80	12.55	14.55	14.65	15.55	20.25	25.55
90	14.13	11.35	18.35	16.78	23.23	30.31
100	10.25	15.55	22.55	18.51	25.55	32.44

Table 2 given above illustrates the performance of FN-BWF method, ACSWF and Validation of EVM with respect to different number of satellite and natural images with varying sizes to measures the average processing time. From the table it is clear that the average processing time is not linear. This is because of the presence of noise is not similar for different images and varies. Hence, a non-linearity is found in the average processing time also. However, the average processing time is found to be lower using FN-BWF method when applied with both the satellite and natural images. This is because of the application of two different algorithms, namely, Function-approximate Discrete Wavelet Transform for preprocessing and Filter Normalized Butterworth Image Denoising (FNBID) algorithm for image denoising. By applying FDWT algorithm, during preprocessing, the edges are said to be preserved. Followed, by which when applied with the FNBID algorithm, denoising is said to be performed in an efficient manner. With the objective of preserving the edges during preprocessing, only the relevant portions of the images are said to be analyzed. Besides, with the edge preserved images, the non relevant portions of the images are not considered during image denoising. For that reason, the FN-BWF method produce a better solution, resulting in the improvement of average processing time than compared to ACSWF¹ and Validation of EVM². In this way, the average processing time is found to be improved by 15% compared to ACSWF and 27% compared to Validation of EVM using satellite images. In a similar manner, the average processing time is found to be improved by 36% compared to ACSWF and 41% compared to Validation of EVM using natural images.

b. Impact of image denoising accuracy

Finally, the third parameter considered for experimentation is the image denoising accuracy. With this metric, the image quality is assessed. The image quality assessment is more efficient if the image denoising accuracy is found to be higher. The image denoising accuracy depends on the proper denoising of the image. It is mathematically evaluated as given below.

$$ID_{acc} = \left[\frac{I_{DC}}{k} \right] * 100 \tag{15}$$

The image denoising accuracy ‘ ID_{acc} ’, is measured on the basis of number of images given as input ‘ k ’, and the images that are correctly denoised, ‘ I_{DC} ’. The sample calculation is provided below, followed by which graphical representation is included.

Sample calculation

- **Proposed FN-BWF:** With ‘10’ satellite images given as input and ‘8’ images being correctly denoised, the image denoising accuracy is as given below.

$$ID_{acc}(\text{using satellite image}) = \left[\frac{8}{10} \right] * 100 = 80\%$$

- **ACSWF:** With ‘10’ satellite images given as input and ‘7’ images being correctly denoised, the image denoising accuracy is as given below.

$$ID_{acc}(\text{using satellite image}) = \left[\frac{7}{10} \right] * 100 = 70\%$$

- **Validation of EVM:** With ‘10’ satellite images given as input and ‘6’ images being correctly denoised, the image denoising accuracy is as given below.

$$ID_{acc}(\text{using satellite image}) = \left[\frac{6}{10} \right] * 100 = 60\%$$

Table 3 :Image denoising accuracy (for satellite images)

No. of images	Image denoising accuracy (for satellite images)		
	FN-BWF	ACSWF	Validation of EVM
10	80	70	60
20	70	60	50
30	70	60	50
40	80	60	60
50	80	70	60
60	70	60	70
70	60	50	50
80	70	60	60
90	80	60	60
100	80	70	70

Finally, the third goal of the experiment is addressed using the image denoising accuracy by showing the comparison between FN-BWF, ACSWF and Validation of EVM respectively. In table 3 the analysis of image denoising accuracy is illustrated with respect to number of images in the range of 10 to 100, involving different sizes. It is measured in terms of percentage (%). As provided in the table, the image denoising accuracy is not directly proportional to the number of satellite images provided as input. In other words, with the increase in the number of satellite images provided as input, the image denoising accuracy is not always increased or decreased. This is because of the varying noise level present in different images. However, comparative analysis shows betterment using the proposed FN-BWF method. This is because of three reasons. First, during preprocessing, the edges are preserved by applying the function approximation with respect to the samples provided as input. Next, with the edge preserved images, discrete wavelet transform is applied using the cut off frequency derived from the mutual information between pixels and the adjacent pixels. Due to

this, only the relevant pixel portions of the images with edges being preserved are obtained. Finally, to this, resultant images, filter normalized Butterworth is applied. With the normalization of filter, image denoising is said to be ensured using the FN-BWF method. This is due to the fact that FN-BWF method considers both preserving the edge and noise removal, while ACSWF and Validation of EVM makes multiple passes in search of noise removal. As a result, the image denoising accuracy is improved by 20% compared to ACSWF and 26% compared to Validation of EVM respectively, when applied with satellite images.

CONCLUSION

In this work, Filter Normalized Butterworth Wavelet Frame (FN-BWF) transforms to noisy satellite and natural for image denoising is presented. The FN-BWF method first performs preprocessing with the objective of preserving the edges by applying the Function Approximation. With this objective, window centered positioning for each sample images are obtained by evaluating the slope values. This in turn minimizes the preprocessing time. Next, with the edge preserved images retrieved, Filter Normalized Butterworth Wavelet Transform is used to perform image denoising. Here, to the edge preserved images, image sharpening is performed so that image contrast is said to be achieved, that in turn helps in the process of image denoising. The image sharpening is performed according to a cut off frequency, different for different samples. This in turn minimizes the significant amount of noise and hence the peak signal to noise ratio is said to be improved. Finally, by applying the filter normalized Butterworth, denoising is said to be achieved in an efficient manner, therefore improving the rate of image denoising accuracy. Experimental results demonstrate that the proposed FN-BWF method not only leads to noticeable improvement over average processing time for image denoising, but also outperforms the image denoising accuracy for both satellite and natural images over methods, namely, ACSWF and Validation of EVM respectively.

REFERENCES

1. Shilpa Suresh, Shyam Lal , Chen Chen, and Turgay Celik, “Multispectral Satellite Image Denoising via Adaptive Cuckoo Search-Based Wiener Filter”, IEEE Transactions on Geoscience and Remote Sensing, Volume: 56 , Issue: 8 , Aug. 2018.
2. Walaa Sahyoun, Jean-Marc Duchamp, and Philippe Benech, “Validation of EVM Method for Filter Test Using Butterworth and Chebyshev Filters”, IEEE Transactions on Microwave Theory and Techniques March 2016; 64(3) – Validation of Error Vector Magnitude (Validation of EVM)²

3. Gasper Tkacik, Patrick Garrigan, Charles Ratliff, Grega Milcinski, Jennifer M. Klein, Lucia H. Seyfarth, Peter Sterling, David H. Brainard, Vijay Balasubramanian, “Natural Images from the Birthplace of the Human Eye”, PLoS ONE, June 2011; 6(6).
4. Olufemi A. Omitaomu, Vladimir A. Protopopescu, Auroop R. Ganguly,” Empirical Mode Decomposition Technique with Conditional Mutual Information for Denoising Operational Sensor Data”, IEEE SENSORS JOURNAL, OCTOBER 2011; 11(10).
5. Wei Zhang, Jiaojie Li, Yupu Yang, “ A fractional diffusion-wave equation with non-local regularization for image denoising”, Signal Processing, Elsevier, Nov 2013
6. Jeny Rajan, Arnold J. den Dekker, Jan Sijbers, “A new non-local maximum likelihood estimation method for Rician noise reduction in magnetic resonance images using the Kolmogorov–Smirnovtest”, Signal Processing, Elsevier, Dec 2013
7. Ashish Phophalia, Ajit Rajwade, Suman K. Mitra, “Rough set based image denoising for brain MR images”, Signal Processing, Elsevier, Feb 2014
8. RuomeiYan, LingShao, LiLiu, YanLiu, “Natural image denoising using evolved local adaptive filters”, Signal Processing, Elsevier, Dec 2013
9. Yue Wu, Brian H. Tracey, Prem kumar Natarajan, Joseph P. Noonan, “Fast blockwise SURE shrinkage for image denoising”, Signal Processing, Elsevier, Jan 2014
10. Khaled Sahnoun, “Satellite Image Compression Technique Using Noise Bit Removal and Discrete Wavelet Transform”, Journal of Multimedia Processing and Technologies, March 2018; 15(1).
11. Praveen Bhargava, Shruti Choubey, Rakesh Kumar Bhujade, Nilesh Jain, “Image Denoising Using Discrete Wavelet Transform: A Theoretical Framework”, International Journal of Engineering & Technology, Feb 2018-10-04
12. Xin Sun, Ning He, Yu-Qing Zhang, Xue-Yan Zhen, Ke Lu, and Xiu-Ling Zhou, “Color Image Denoising Based on Guided Filter and Adaptive Wavelet Threshold”, Applied Computational Intelligence and Soft Computing, Nov 2017,
13. Kai Zhang, Wangmeng Zuo, Yunjin Chen, Deyu Meng, and Lei Zhang, “Beyond a Gaussian Denoiser: Residual Learning of Deep CNN for Image Denoising”, IEEE TRANSACTIONS ON IMAGE PROCESSING, JULY 2017; 26(7).
14. Qi Ge, Xiao-Yuan Jing, Fei Wu, Zhi-hui Wei, Liang Xiao, Wen-Ze Shao, Dong Yue, Hai-bo Li, “Structure-based Low-Rank Model with Graph Nuclear Norm Regularization for Noise Removal”, IEEE Transactions on Image Processing July 2017;26(7).
15. Vadim Fedorov, and Coloma Ballester, “Affine Non-local Means Image Denoising”, IEEE Transactions on Image Processing May 2017; 26(5).

16. Tao Huang, Weisheng Dong, Xuemei Xie, Guangming Shi, Xiang Bai, “Mixed Noise Removal via Laplacian Scale Mixture Modeling and Nonlocal Low-rank Approximation”, IEEE Transactions on Image Processing July 2017; 26(7).
 17. Norbert Remenyi, Orietta Nicolis, Guy Nason, and Brani Vidak, “Image Denoising With 2D Scale-Mixing Complex Wavelet Transforms”, IEEE TRANSACTIONS ON IMAGE PROCESSING, DECEMBER 2014;23(12).
 18. B. H. Tracey, E. L. Miller, Y. Wu, P. Natarajan, J. P. Noonan, “A constrained optimization approach to combining multiple non-local means denoising estimates”, Signal Processing, Elsevier, Dec 2013
 19. Zhaojun Yuan, Xudong Xie, Jianming Hu, Danya Yao, “An Efficient Method for Traffic Image Denoising”, International Conference on Traffic & Transportation Studies (ICTTS’2014), Elsevier, Feb 2014
 20. Ayush Dogra and Parvinder Bhalla, “Image Sharpening By Gaussian And Butterworth High Pass Filter”, Biomedical & Pharmacology Journal, Nov 2014
 21. RigDas., and Themrichon Tuithung., “A Novel Steganography Method for Image Based on Huffman Encoding”, IEEE Transaction on Image Processing, June 2012
-